Published in : Fire Technology (2010)
Status : Postprint (Author's version)

Numerical Modelling of Thin-Walled Stainless Steel Structural Elements in Case of Fire

Nuno Lopes and Paulo Vila Real, Department of Civil Engineering, LABEST - University of Aveiro, 3810-193 Aveiro, Portugal
Luis Simδes da Silva, Department of Civil Engineering, ISISE – University of Coimbra, 3030 Coimbra, Portugal
Jean-Marc Franssen, Structural Engineering, University of Liege, Liege, Belgium

Abstract. In this paper, the structural response of stainless steel thin-walled elements submitted to fire is analysed numerically by means of the geometrically and materially non-linear Finite Element program SAFIR, including imperfections. In order to make these simulations, two main changes in the program were made: (i) the code was changed in order to deal with the stainless steel 2D material constitutive law to be used with shell elements and (ii) the possibility of the program to take into account residual stresses with shell finite elements was introduced. The stainless steel stress-strain relationship at high temperatures was based on the one presented in part 1.2 of Eurocode 3. To model the strain hardening exhibited by the stainless steels, using the shell element formulation, an approximation to the Eurocode 3 constitutive law was needed. Local and global geometrical imperfections were considered in the simulations. The paper shows the influence of the residual stresses on the ultimate load-carrying capacity of thin-walled stainless steel structural elements in case of fire.

Keywords: stainless steel, fire, thin-walled, numerical modelling, local buckling

Nomenclature

a, b, c, d Parameters to calculate the stainless steel stress-strain relationship: and also parameters to calculate the approximation proposed in this paper to the stainless steel hardening rule
e Parameter to calculate the stainless steel stress-strain relationship
$f_{u,\theta}$ Tensile strength
$f_{0.2p,\theta}$ The proof strength at 0.2% plastic strain
k Plastic strain
$E_{a,\theta}$ Slope of the linear elastic range
$E_{a,\theta}$ Slope of the linear elastic range
$E_{ct,\theta}$ Slope at proof strength
$\varepsilon_{c,\theta}$ Total strain at proof strength
$\varepsilon_{u,\theta}$ Ultimate strain
σ_1, σ_2 Principal stresses
$\sigma_{c,res}$ Comparison stress of the residual stresses
τ Stress from the hardening rule
$\{\sigma_{res}\}$ Matrix of residual stresses in the axis i (x, y and xy)
$\{\varepsilon_{res}\}$ Matrix of residual strains in the axis i (x, y and xy)

1. Introduction

Stainless steel has various desirable characteristics for a structural material [1-3]. But, even if its use in construction is increasing, it is nevertheless still necessary to develop the knowledge on its structural behaviour, especially at elevated temperatures. Stainless steels are known by their non-linear stress-strain relationships with a low limit of proportionality and an extensive hardening phase. Well defined yield strength does not exist, therefore the conventional limit of elasticity at 0.2% is usually considered in simple calculations.

EN 1993-1-4 "Supplementary rules for stainless steels" [4] gives design rules for stainless steel structural members at ambient temperature. In this part of Euro-code 3, the assessment of the stainless steel fire resistance is referred to the fire part of the same Eurocode (EN 1993-1-2) [5], where it is stated that the design guidelines for carbon steel elements may be used for stainless steel elements. However, these two materials have rather different mechanical properties at elevated temperatures as Figure 1 shows the stress-strain relationship of stainless steel 1.4301 at 600°C is here compared to the carbon steel stress-strain relationship at the same temperature, according to the prescriptions of part 1.2 of Eurocode 3.

The program SAFIR [6], a geometrical and material non linear finite element code especially developed to model the behaviour of structures in case of fire, has been used in the numerical simulations. This program has been adapted according to the material properties defined in EN 1993-1-4 [4] and EN 1993-1-2 [5] to model the behaviour of stainless steel structures.

Figure 1. Stress-strain relationships of carbon steel S 235 and stainless steel 1.4301 at 600°C.

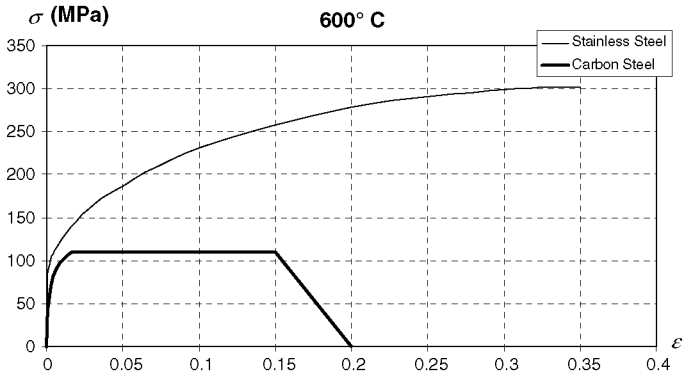

An approximation to the Eurocode 3 constitutive law [5] for the stainless steel was introduced due to the fact that the stainless steel stress-strain relationship cannot be analytical inverted as it will be explained latter.

As the program takes into account the residual stresses by transforming them first into residual strains and adding them after to the other initial strains [7], it was necessary to implement a procedure that makes this conversion considering the non-linearity of the stainless steel stress-strain relationship.

The objective of the study presented in this paper is to evaluate the accuracy of the hardening rule introduced for the shell finite elements in the program SAFIR and to study the influence of the residual stresses in thin-walled stainless steel cross-sections.

2. Software Development

The main changes made in the program were:
- changing the program in order to deal with stainless steel 2D constitutive model, to be used with shell finite elements;
- introducing the possibility to take into account residual stresses in shell elements for stainless steel.

2.1. Implementation of the Stainless Steel 2D Material Constitutive Law

The modelling of stainless steel was made by a non-elastic plane stress condition, based on the von Mises surface and isotropic hardening. The constitutive law of stainless steel has no elastic domain.

The implemented shell finite element was programmed to be used in large displacements in the context of plane stress condition. This finite element was first introduced for elastic materials and then for bi-dimensional elasto-plastic constitutive law [8].

Table 1: Expressions of the Constitutive Law of the Stainless Steel at High Temperatures [5]

Strain range	Stress σ	Tangent modulus
$\varepsilon \le \varepsilon_{c,\theta}$	$\frac{E\cdot\varepsilon}{1+a\cdot\varepsilon^b}$	$\frac{E\left(1+a\cdot\varepsilon^b-a\cdot b\cdot\varepsilon^b\right)}{\left(1+a\cdot\varepsilon^b\right)^2}$
$\varepsilon_{c,\theta} < \varepsilon < \varepsilon_{u,\theta}$	$f_{0.2p,\theta} - e + (d/c)\sqrt{c^2 - \left(\varepsilon_{u,\theta} - \varepsilon\right)^2}$	$\frac{d\left(\varepsilon_{u,\theta}-\varepsilon\right)}{c\sqrt{c^2-\left(\varepsilon_{u,\theta}-\varepsilon\right)^2}}$
Parameters	$\varepsilon_{c,\theta} = f_{0.2p,\theta}/E_{a,\theta} + 0.002$	
Functions	$a = \frac{E_{a,\theta}\varepsilon_{c,\theta}-f_{0.2p,\theta}}{f_{0.2p,\theta}\varepsilon_{c,\theta}}$	$b = \frac{1-\left(\varepsilon_{c,\theta}E_{ct,\theta}/f_{0.2p,\theta}\right)E_{a,\theta}\varepsilon_{c,\theta}}{\left(E_{a,\theta}\varepsilon_{c,\theta}/f_{0.2p,\theta}-1\right)f_{0.2p,\theta}}$
	$c^2 = \left(\varepsilon_{u,\theta} - \varepsilon_{c,\theta}\right)\left(\varepsilon_{u,\theta} - \varepsilon_{c,\theta} + \frac{e}{E_{ct,\theta}}\right)$	$d^2 = e(\varepsilon_{u,\theta} - \varepsilon_{c,\theta})E_{ct,\theta} + e^2$
	$e = \frac{\left(f_{u,\theta}-f_{0.2p,\theta}\right)^2}{\left(\varepsilon_{u,\theta}-\varepsilon_{c,\theta}\right)E_{ct,\theta}-2\left(f_{u,\theta}-f_{0.2p,\theta}\right)}$	

The same formulation used in the carbon steel [8] was used for the stainless steel, but, due to the impossibility of inverting the stress-strain relationship (see Table 1) for the first branch of the curve ($\varepsilon < \varepsilon_{c,\theta}$), an approximation had to be used.

The stainless steel stress-strain relationship introduced in the program fits with the one prescribed in part 1.2 of Eurocode 3 [5] for uniaxial relationship described in Table 1 and in Figure 2.

The constitutive law given by the function $\sigma = \sigma(\varepsilon)$ can be found in Table 1. The implemented hardening rule, $\tau = \tau(k)$, was obtained using $\varepsilon = k + \frac{\sigma}{E}$ and making $\tau = \sigma$ (see Figure 2).

For the second branch ($\varepsilon_{c,\theta} \le \varepsilon \le \varepsilon_{u,\theta}$) it was possible to use this procedure to achieve directly the hardening rule, but for $\varepsilon < \varepsilon_{c,\theta}$ the equation $\sigma = E\ .\varepsilon/(1 + a\ .\ \varepsilon^b)$ cannot be inverted. Therefore, the Equation (1), approximating the hardening function for the first branch of the stainless steel constitutive law, was developed.

$$\tau = b \cdot k^2 + c \cdot k + d + a \cdot \sqrt{k} \qquad (1)$$

The parameters *a, b, c* and *d* were obtained imposing that Equation (1) should satisfy the boundary conditions at both ends of the curve ($0 < \varepsilon < \varepsilon_{c,\theta}$), resulting in

$$\begin{cases} a = 56.0362 \cdot f_{0.2p,\theta} - 0.112 \cdot h \\ b = 63501.9 \cdot f_{0.2p,\theta} - 127.1 \cdot h \\ c = -880.512 \cdot f_{0.2p,\theta} + 2.763 \cdot h \\ d = 0.001 \cdot f_{0.2p,\theta} \end{cases} \qquad (2)$$

where h is the value of $\frac{\partial\tau}{\partial k}(0.002)$ in the second branch.

Figure 3 shows a comparison between the stress-strain relationship obtained with Eurocode 3 and the Equation (1). A very good agreement between the two curves can be observed.

2.2. Introduction of Residual Stresses Using Shell Finite Elements

In order to introduce the possibility of taking into account residual stresses it is necessary first to transform them into residual strains and after to add them to the other initial strains [7].

Due to this procedure, for inelastic materials, as it is the case of stainless steel, plastic strains, corresponding to the residual stresses (as shown in Figure 4) must be evaluated according to:

$$\varepsilon_{res} = \varepsilon_{res}^{el} + \varepsilon_{res}^{pl} = \frac{\sigma_{res}}{E_0} + \varepsilon_{res}^{pl} \tag{3}$$

The procedure is trivial with materials that have an initial linear elastic phase provided that the residual stresses are always in this elastic phase.

With non linear materials, the procedure starts with the determination of a "comparison stress" of von Mises (see Equation 3) of the introduced residual stresses.

$$\sigma_{c,res} = \sqrt{\sigma_{x,res}^2 - \sigma_{x,res} \cdot \sigma_{y,res} + \sigma_{y,res}^2 + 3 \cdot \tau_{xy,res}} \tag{4}$$

With this "comparison stress" and with the constitutive law described in Sect. 2.1 it is possible, using an iterative procedure, to achieve a residual "comparison strain". In this work the Newton-Raphson method was adopted.

With the comparison residual strain and with the comparison residual stress it is possible to determine a secant modulus $E_{sec} = \sigma_{c,res}/\varepsilon_{c,res}$@. This modulus is used in the elasticity matrix *[D]* necessary to evaluate the residual strains.

$$\{\varepsilon_{res}\} = [D]^{-1} \cdot \{\sigma_{res}\} \tag{5}$$

A similar procedure, for inelastic materials, is used in the Finite Element package ABAQUS, where the plastic strains corresponding to the residual stresses are introduced by means of a special subroutines [9].

Figure 2. Stress-strain relationship of the stainless steel at elevated temperatures.

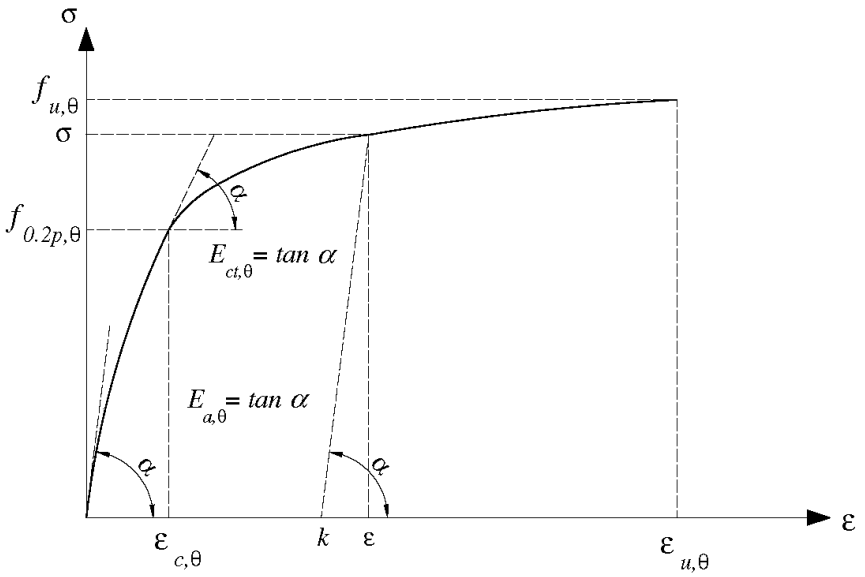

Figure 3. Stainless steel first branch of the constitutive law: comparison between the implemented approximation and the EC3 (EN 1993-1 -2) at 600°C, for the stainless steel grade 1.4301.

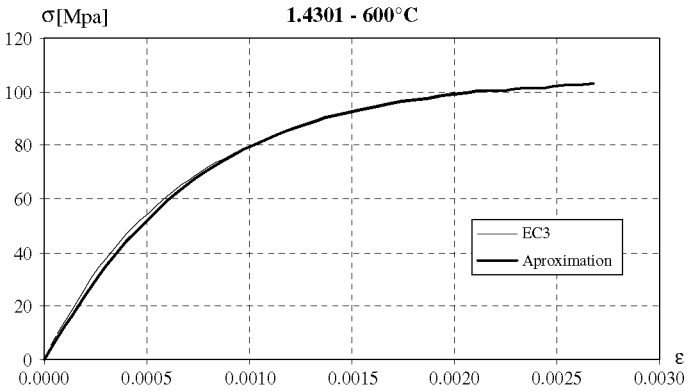

Figure 4. Consideration of residual strains in non-linear constitutive laws.

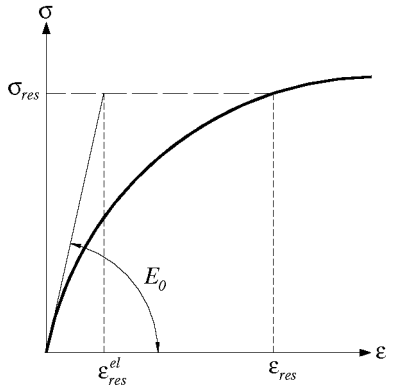

3. Validation of the Software Development

The results of the developments made in the shell finite elements of the program SAFIR are compared in this section with the results of the 3D beam finite element of the same program, with the 3D beam finite element of the commercial software ANSYS and with some experimental tests made by Ala-Outinen et al. [10].

Comparisons are made for elements with Class 1 sections. The flexural buckling of a square hollow section and the lateral-torsional buckling of an I-cross section are analysed with shell and beam finite elements.

3.1. Flexural Buckling of a Class 1 Stainless Steel Square Hollow Section

To check the accuracy of the recent developments, the same Class 1 hollow section SHS 40 x 40 x 4 used in reference [10] in experimental tests on stainless steel columns in case of fire has been used in this study. The round corners were not considered in the finite element mesh used to discretize the cross-section.

A lateral geometric imperfection, in accordance with the permitted tolerance in EN 1090 [11] given by the following expression was considered

$$y(x) = \frac{l}{1000}\sin\left(\frac{\pi x}{l}\right) \qquad (6)$$

where l is the length of the column. Figure 5 shows the deformed shape of the column immediately before the collapse.

Figure 5. SHS 40 x 40 x 4 column simulated with shell elements (x5).

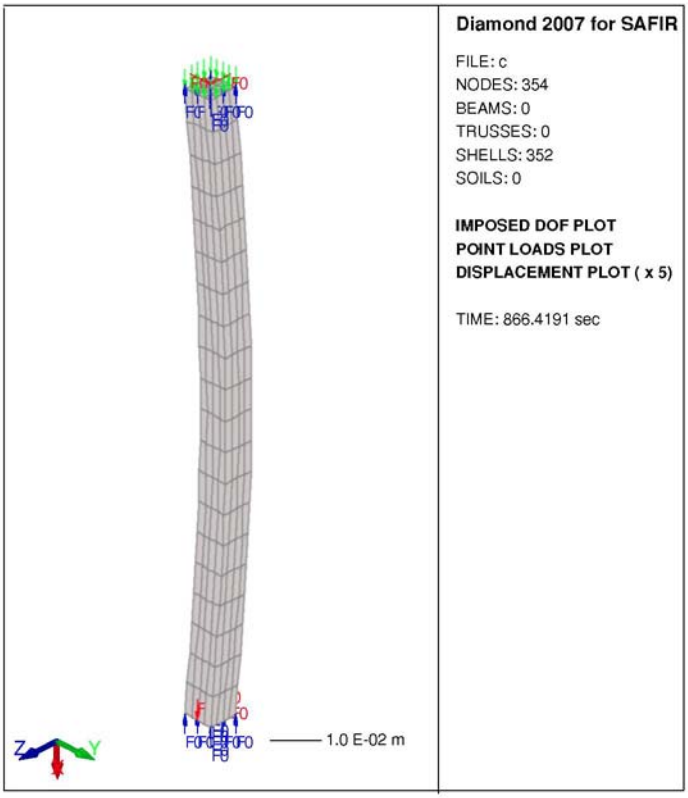

No residual stresses were introduced in these first simulations. The yield strength and the ultimate strength considered were 210 MPa and 520 MPa respectively. It wasn't considered the increasing of the yield strength in the corner regions derived from cold working [12]. The comparisons were made with uniform temperature in the cross-section.

Figure 6 shows the results obtained for 500°C using the beam finite element from SAFIR and from ANSYS. These results are compared with the Eurocode 3 simple design method (denoted "EN 1993-1-2").

To compare the numerical results with the experimental tests made by Ala-Outinen et al. [10] the same yield strength and the ultimate strength measured in the tests of 595 MPa and 736 MPa respectively, were used in the results presented in Figure 7. The load level, the length and the support conditions of the numerical simulations correspond to the ones that are present in the experimental tests. In Figure 7, "Outinen tests" correspond to the experimental tests, "Outinen tests

Figure 6. SHS 40 x 40 x 4 numerical results using 3D beam finite elements.

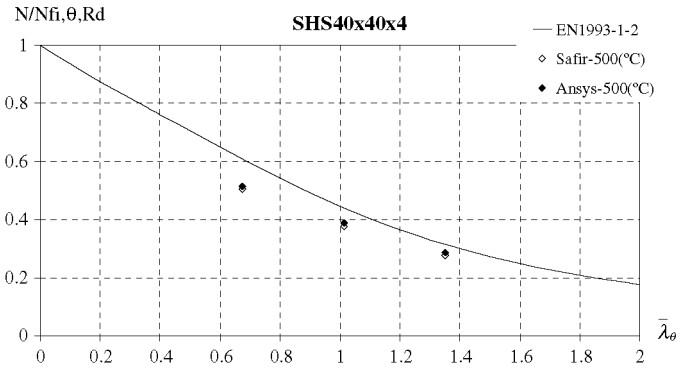

Figure 7. SHS 40 x 40 x 4 numerical results with SAFIR using beam and shell finite elements compared with the experimental tests [9].

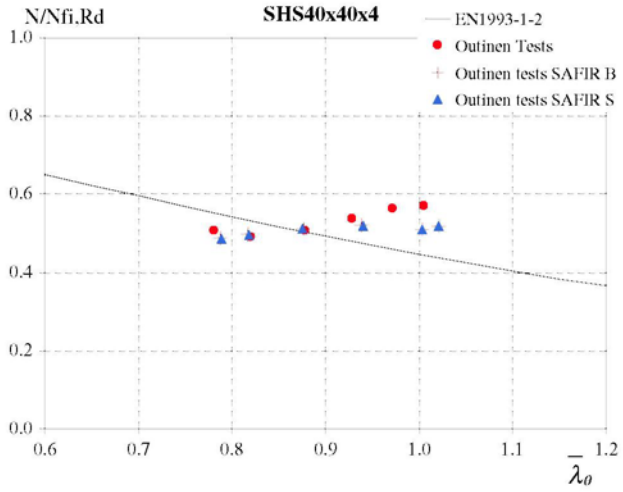

SAFIR B" are the simulations of the experimental tests with the beam elements and "Outinen tests SAFIR S" are the simulations of the experimental test with the shell elements.

The results shown in Figure 7 were obtained for different steel temperatures in the range of 500-900°C.

From Figures 6 and 7 it can be concluded that the approximation used for the stainless steel hardening rule implemented in SAFIR gives good approximation when compared with the results from others software and with experimental results.

A second study with the SHS 40 x 40 x 4 columns to evaluate the influence of the residual stresses was made.

Figure 8. Residual stresses in a hollow section: C compression, T tension [13].

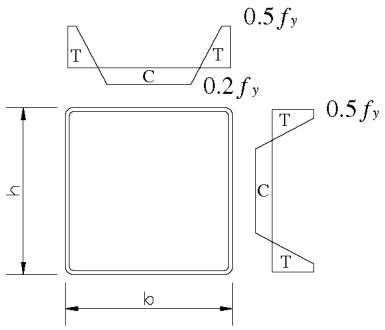

The adopted residual stresses were considered as constant across the thickness of the internal section members. For the square hollow section, the pattern shown in Figure 8 [13] was used.

Adopting the same methodology used by Gardner and Nethercot [14], prior to the application of external loading, a preliminary load step to allow equilibration of the residual stresses was made.

Table 2 compares the results obtain with beam elements, shell element and the simple formulae from the Eurocode 3.

Table 2 also shows that the Eurocode 3 is not in the safe side when compared with the numerical simulations. It is also possible to conclude that the residual stresses have a little influence on the ultimate load carrying capacity, being in accordance with the conclusions from other authors [9, 14].

3.2. Lateral-Torsional Buckling of a Class 1 Stainless Steel Equivalent IPE Welded Section

In this section a comparison between the results obtained using the 2D constitutive law for shell elements with the results obtained using 3D beam elements, with and without residual stresses, is presented.

It was chosen to test a simply supported beam subjected to uniform bending moment with Class 1 cross-section, a welded equivalent IPE 220 cross-section (see Figure 9). In the numerical simulations, a lateral geometric imperfection given by expression (6) was considered. The adopted yield strength and the ultimate strength were 210 MPa and 520 MPa respectively. The comparisons were made considering a uniform temperature of 600°C in the cross-section.

The adopted residual stresses are considered as constant across the thickness of the webs and flanges. For the welded IPE section, the distribution shown in Figure 10, that has the maximum value of f_y (yield strength) [15] was used.

From Table 3 it can be again concluded that the introduction of the residual stresses in shell elements, gives results that are in good agreement with the results obtained with the 3D beam elements. Again the influence of the residual stresses on the ultimate load carrying capacity is negligible.

Table 2. Results for the Hollow Section

		Without residual stresses	With residual stresses	With/without residual stresses	EN 1993-1-2
L= 2 m	Beam	23.1 kN	22.8 kN	0.99	26.9 kN
	Shell	22.9 kN	22.7 kN	0.99	
L = 3 m	Beam	13.4 kN	12.6 kN	0.94	14.8 kN
	Shell	13.1 kN	12.7 kN	0.97	

Figure 9. Simply supported stainless steel beam subjected to uniform bending.

Figure 10. Residual stresses in an IPE welded section: C compression, T tension.

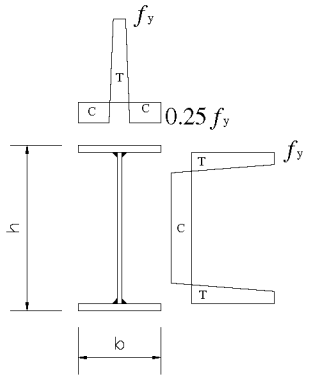

Table 3. Results for the l-Section

		Without residual stresses	With residual stresses	With/without residual stresses	EN 1993-1-2
L = 3 m	3D-Beam	20.6 kNm	19.9 kNm	0.97	20.3 kNm
	Shell	19.3 kNm	19.2 kNm	0.99	
L = 5 m	3D-Beam	15.7 kNm	15.0 kNm	0.96	14.1 kNm
	Shell	14.3 kNm	14.0 kNm	0.98	

4. Influence of the Residual Stresses in Class 4 Stainless Steel Sections

In this section two examples representative of thin-walled steel members applications are presented. The first one is an axially loaded square hollow section and the second is a plate girder, both with Class 4 cross-section.

4.1. Residual Stresses in Axially Loaded Class 4 Square Hollow Sections

In order to study the influence of the residual stresses in axially loaded thin-walled sections, a numerical study with two square hollow Class 4 sections is presented in this section. In this study the magnitude of the imperfections was chosen to be *b/* 200 [16] for the local imperfections and *l*/1000 [17] for the global imperfections, typical values used in the study of thin-walled structural elements [18], and prescribed in the part 1.5 of Eurocode 3 [16].

Numerical results obtained for columns with the square hollow sections SHS 150 x 150 x 3 and SHS 200 x 200 x 5 of the stainless steel grade 1.4301 are presented. The yield strength and the ultimate strength considered were 210 MPa and 520 MPa respectively. The comparisons were made with uniform temperature of 600°C in the cross-section. The tested columns had lengths of 0.9 m with fixed ends and were subjected to centric axial compression (see Figure 11). This length was chosen so that the collapse would be by local buckling instead of global buckling. In these numerical tests the curvature of the corners was considered.

For the tested columns without residual stresses it was considered the following possibilities:

(a) no geometric imperfections and no higher corners yield strength derived from cold working;

(b) no geometric imperfections but introducing higher corners yield strength according to Ashraf and Gardner et al. [12];

(c) global imperfections given by expression (6) and introducing higher corners yield strength;

(d) local imperfections with a maximum value of *b/200* [16] and introducing higher corners yield strength;

(e) global imperfections given by expression (6), local imperfections with a maximum value of *b/200* and introducing higher corners yield strength.

Figure 11. Column with α thin-walled stainless steel hollow section.

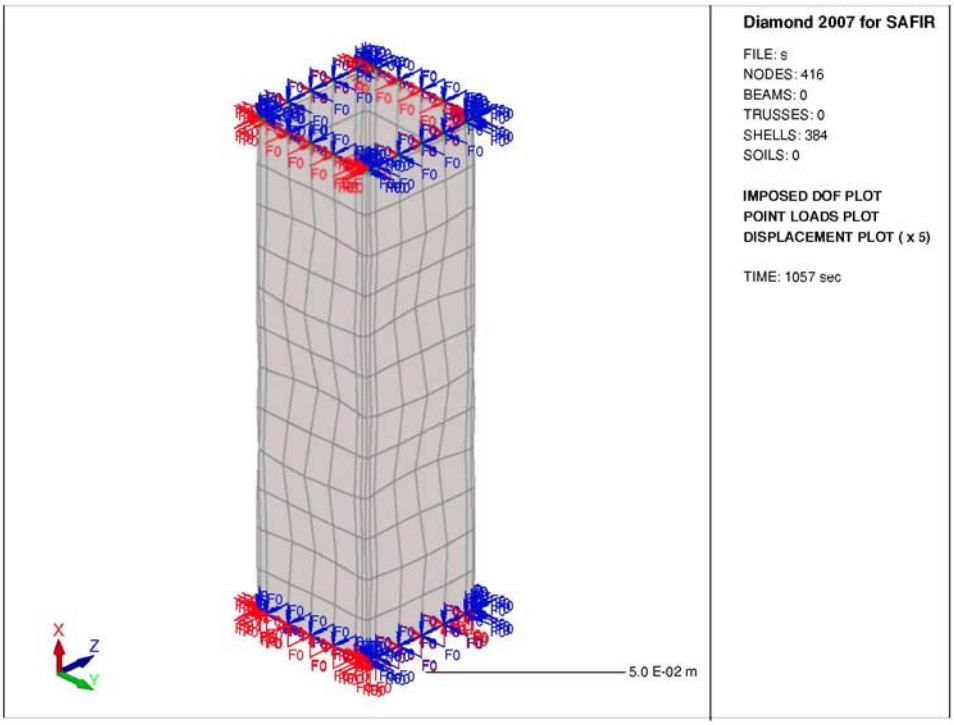

Table 4 shows the corresponding numerical results of these five analysed cases.

Table 4 shows that no global imperfections are needed to be considered when local buckling is the main failure mode. Therefore, in the results shown in Table 5 the residual stresses were introduced only in the case (d).

For the square hollow section, the distribution shown in Figure 8 [13] was used.

Table 5 shows the obtained results for columns with local imperfections, with and without residual stresses.

From these results it can be concluded that the influence of the residual stresses is small. However this influence is of the same magnitude of the one observed in Table 2 for a Class 1 section. The results from EC3 are in good agreement with the numerical results.

Table 4. Ultimate Axial Compression Effort Without Residual Stresses

Case	SHS 150 x 150 x 3	SHS 200 x 200 x 5
a	160.5 kN	423.8 kN
b	175.5 kN	473.6 kN
c	174.5 kN	465.6 kN
d	149.5 kN	387.9 kN
e	149.5 kN	387.9 kN

Table 5. Ultimate Axial Compression Effort with Local Imperfections

	SHS 150 x 150 x 3	SHS 200 x 200 x 5
Without residual stresses	149.5 kN	387.9 kN
With residual stresses	139.5 kN	376.5 kN
With/without residual stresses	0.93	0.97
EN 1993-1-2	136.9 kN	356.8 kN

4.2. Residual Stresses in Class 4 I-Sections in Bending

In order to achieve a shape for the local imperfections it was made a modal analysis with the program CUFSM [19] considering the beam submitted to a normal stresses diagram correspondent to bending. This program was developed by Scha-fer [19] to determine the elastic buckling and corresponding modes of thin-walled structural elements.

The program CUFSM uses the finite strip method [11]. When a cross-section is defined, with a stress condition, the program makes the analysis of different lengths for the section. The stress and the shape of each buckling mode are recorded for each of the lengths [20].

Figure 12 shows the first buckling mode of the studied I cross-section. This first buckling mode shape was used for the shape of the initial local imperfections, with the maximum of *b*/200 (being *b* the height of the web).

Numerical results obtained for beams with the I-sections 900 x 300 x 9 (height x base x thickness) and 800 x 250 x 8 of the stainless steel grade 1.4301 will be shown. The yield strength and the ultimate strength considered were 210 MPa and 520 MPa respectively. The comparisons were made with uniform temperature of 600°C in the cross-section for simply supported beams with 2.0 m of length, fork supports and submitted to uniform bending. Figure 13 shows the deformed shape immediately before the collapse. The adopted length was chosen so that the collapse would be by local buckling instead of global buckling.

Figure 12. First buckling mode obtained with the program CUFSM [16].

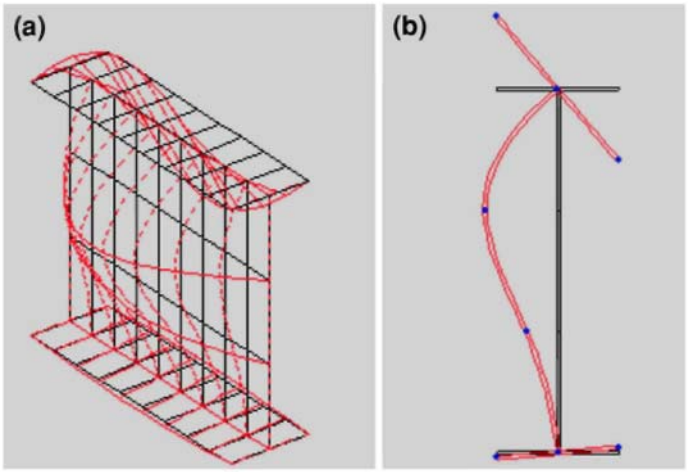

For the tested beams without residual stresses it was considered the following possibilities:

(a) no geometric imperfections;

(b) only global imperfections given by expression (6);

(c) only local imperfections with a maximum value of *b/200;*

(d) global imperfections given by expression (6) and local imperfections with a maximum value of *b/200*.

From Table 6 it can be concluded that no global imperfections are needed to be considered in this case, due to the fact that the collapse occurs by local buckling.

Figure 13. Stainless steel beam analysed with shell elements.

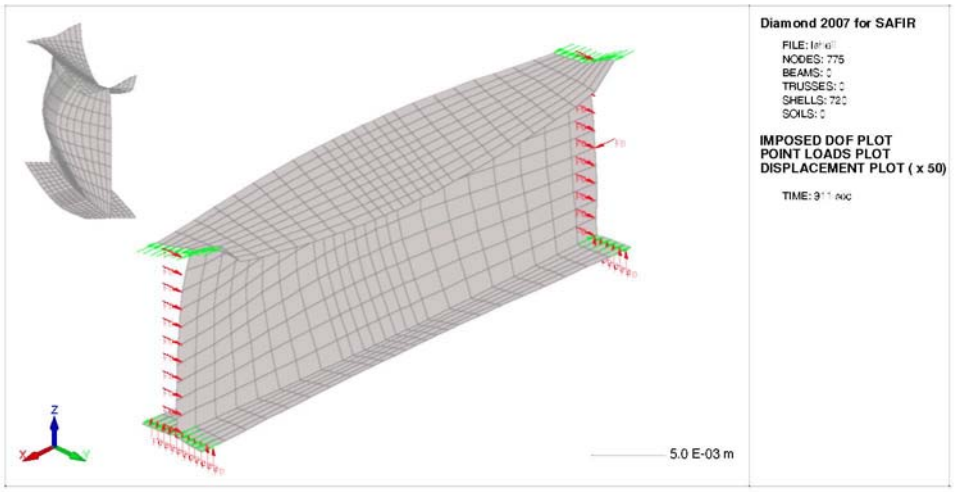

Table 6. Ultimate Bending Moment Effort Without Residual Stresses

Case	I 900 x 300 x 9	I 800 x 250 x 8
a	251 kNm	169 kNm
b	249 kNm	167 kNm
c	227 kNm	156 kNm
d	226 kNm	156 kNm

The pattern of residual stresses distribution shown in Figure 10 [13] was used. Only residual stresses with the direction of the longitudinal axis of the beam were considered *($\sigma_{x,res}$)*. Prior to the application of external loading, a preliminary load step to allow equilibration of the residual stresses was made. Figure 14 shows the normal force field corresponding to this equilibrated stresses state before any external loading be applied and the corresponding principal stress directions.

Tables 7 and 8 show the obtained results for the beams with global imperfections and with local imperfections respectively, considering or not residual stresses.

Table 7. Ultimate Bending Moment Effort with Only Global Imperfections

	I 900 x 300 x 9	I 800 x 250 x 8
Without residual stresses	249 kNm	167 kNm
With residual stresses	244 kNm	165 kNm
With/without residual stresses	0.98	0.99
EN 1993-1-2	255 kNm	165 kNm

Figure 14. (a) Normal force field, (b) Principal stress directions.

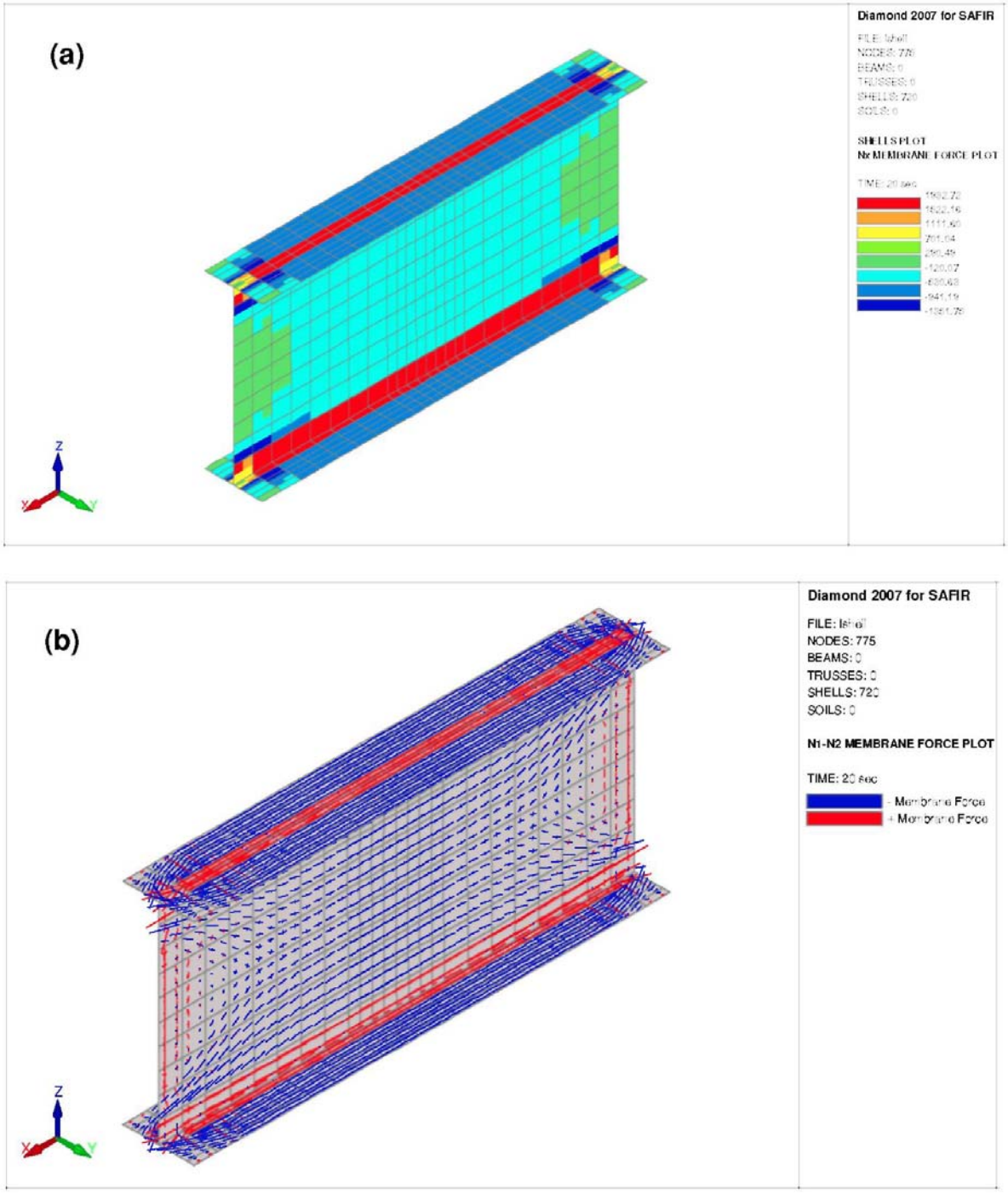

Table 8. Ultimate Bending Moment Effort with Only Local Imperfections

	I 900 x 300 x 9	I 800 x 250 x 8
Without residual stresses	227 kNm	156 kNm
With residual stresses	230 kNm	158 kNm
With/without residual stresses	1.01	1.01
EN 1993-1-2	255 kNm	165 kNm

Paradoxically, Table 8 shows that the inclusion of residual stresses provides a beneficial effect on the ultimate load-carrying capacity. The same conclusions were observed in [9].

From these results it can be concluded that there is very little influence of the residual stresses in the studied bended thin-walled structural elements. From the comparison made with EC3 it can be concluded that it does not give safe approximations to the numerical results.

5. Conclusions

This paper has shown that the implemented approximation in the program SAFIR for the stainless steel hardening law at high temperatures using shell elements, gives good results when compared with the results obtained with beam finite elements.

It was shown that the influence of the residual stresses on the ultimate load carrying capacities of stainless steel Class 4 sections is rather small. However this influence for the studied axially loaded columns is of the same magnitude of the one observed for a Class 1 section, which suggests that the residual stress must be considered for the evaluation of the load-carrying capacity of columns subjected to fire. In the case of the beams the influence of the residual stresses can be neglected.

The paper has also shown that the results from the Eurocode 3 are not on the safe side for structural elements with Class 4 cross-section. It is worth noting that more numerical and experimental tests should be done to confirm the unsafe nature of the Eurocode 3 results and see whether new formula to be used with Class 4 elements should be developed.

Acknowledgements

The authors would like to thank Prof. Paulo Piloto from the Technical University of Braganca for the numerical results obtained with ANSYS.

References

1. Estrada I (2005) Shear design of stainless plate girders. PhD Thesis, Universitat Politec-nica de Catalunya, Barcelona, Spain

2. Gardner L (2005) The use of stainless steel in structures. Prog Struct Eng Mater 7(2):45-55. doi:10.1002/pse.l90

3. Euro Inox and Steel Construction Institute (2006) Design manual for structural stainless steel, 3rd edn. Euro Inox and Steel Construction Institute, London

4. European Committee for Standardisation (2006) EN 1993-1-4 Eurocode 3: design of steel structures—Part 1.4.: general rules—supplementary rules for stainless steels. Brussels, Belgium

5. European Committee for Standardisation (2005) EN 1993-1-2 Eurocode 3: design of steel structures—Part 1.2: general rules—structural fire design. Brussels, Belgium

6. Franssen J-M (2005) SAFIR a thermal/structural program modelling structures under fire. Eng Journal AISC 42(3): 143-158

7. Franssen J.-M. (1993) Residual stresses in steel profiles submitted to the fire: an analogy. In: 3rd CIB/W14 workshop "modelling", TNO building and construction research. Rijswijk, The Netherlands

8. Doneux C, Franssen J-M (2003) 2D constitutive models for the shell elements of the finite element software SAFIR. M&S report, translation of "Rapport interne—SPEC/ 97_01" by C. Doneux. University of Liege, Liege, Belgium

9. Jandera M, Gardner L, Machaceka J (2008) Residual stresses in cold-rolled stainless steel hollow sections. J Constr Steel Res 64:1255-1263. doi:10.1016/j.jcsr.2008.07.022

10. Ala-Outinen T, Oksanen T (1997) Stainless steel compression members exposed to fire, VTT research notes 1864. Espoo, Finland

11. Cheung YK (1976) Finite strip method in structural analysis. Pergamon Press, New York

12. Ashraf M, Gardner L, Nethercot DA (2005) Strength enhancement of the corner regions of stainless steel cross sections. J Constr Steel Res 61(l):37-52

13. ECCS (1984) Ultimate limit state calculation of sway frames with rigid joints, 1st edn

14. Gardner L, Nethercot DA (2004) Numerical modeling of stainless steel structures components—a consistent approach. J Struct Eng (October):1586-1601. doi:10.1061/ (ASCE)0733-9445(2004)130:10(1586)

15. Chen WF, Lui EM (1991) Stability design of steel frames. CRC Press, London

16. European Committee for Standardisation (2006) EN 1993-1-5 Eurocode 3: design of steel structures—Part 1.5: plated structural elements. Brussels, Belgium

17. European Committee for Standardisation (2005) EN 1090-2. Execution of steel and aluminium structures—Part 2: technical requirements for the execution of steel structures. Brussels, Belgium

18. Uppfeldt B, Outinen T, Veljkovic M (2008) A design model for stainless steel box columns in fire. J Constr Steel Res 64(11): 1294-1301

19. Schafer BW (1997) Cold-formed steel behaviour and design: analytical and numerical modeling of elements and members with longitudinal stiffeners. PhD Dissertation, Cornell University, Ithaca

20. Sarawit AT, Kim Y, Bakker MCM, Peko T (2003) The finite element method for thin-walled members-applications. Thin-Walled Struct 41:191-206. doi:10.1016/S0263-8231 (02)00087-3